AIP Applied Physics Letters

Effects of magnetic field and pressure in magnetoelastic stress reconfigurable thin film resonators

M. Staruch, C. Kassner, S. Fackler, I. Takeuchi, K. Bussmann, S. E. Lofland Jr., C. Dolabdjian, R. Lacomb, and P. Finkel

Citation: Applied Physics Letters **107**, 032909 (2015); doi: 10.1063/1.4927309
View online: http://dx.doi.org/10.1063/1.4927309
View Table of Contents: http://scitation.aip.org/content/aip/journal/apl/107/3?ver=pdfcov
Published by the AIP Publishing

APPLIED PHYSICS LETTERS **107**, 032909 (2015)

Effects of magnetic field and pressure in magnetoelastic stress reconfigurable thin film resonators

M. Staruch,[1] C. Kassner,[2] S. Fackler,[3] I. Takeuchi,[3] K. Bussmann,[1] S. E. Lofland, Jr.,[2] C. Dolabdjian,[4] R. Lacomb,[5] and P. Finkel[1]
[1]*Naval Research Laboratory, Washington, DC 20375, USA*
[2]*Department of Physics and Astronomy, Rowan University, Glassboro, New Jersey 08028, USA*
[3]*Department of Materials Science and Engineering, University of Maryland, College Park, Maryland 20742, USA*
[4]*Normandie Univ, France; UCBN, GREYC, F-14032 Caen, France; and CNRS, UMR 6072, F-14032 Caen, France*
[5]*Naval Undersea Warfare Center, Newport, Rhode Island 02841, USA*

(Received 24 June 2015; accepted 12 July 2015; published online 22 July 2015)

Free-standing CoFe thin-film doubly clamped stress reconfigurable resonators were investigated as a function of magnetic field and pressure. A large uniaxial anisotropy resulting from residual uniaxial tensile stress, as revealed from magnetic hysteresis loops, leads to an easy magnetization axis aligned along the length of the beams. The quality factor of the driven resonator beams under vacuum is increased by 30 times, leading to an enhanced signal-to-noise ratio and a predicted reduction in the intrinsic magnetic noise by a factor of 6, potentially reaching as low as $\sim$25 pT/$\sqrt{}$Hz at 1 Torr. Stress reconfigurable sensors operating under vacuum could thus further improve the limit of detection and advance development of magnetic field sensing technology. *© 2015 AIP Publishing LLC*. [http://dx.doi.org/10.1063/1.4927309]

Recent work on magnetoelectric (ME) composites exploiting high coupling between piezoelectric and magnetostrictive phases has established ME materials as very promising candidates for magnetic field sensing. Magnetic field sensors based on ME composites have been demonstrated to exhibit comparable sensitivity and noise floor to magnetometers based on resonant Lorentz force, anisotropic magnetoresistance, or magnetoimpedance.[1–5] The main advantage of ME sensors is that by utilizing the direct effect, i.e., conversion of a magnetic signal to a voltage, they allow for completely passive detection and thus are an ultra-low power alternative to these other devices. By driving these sensors at electromechanical resonance, several orders of magnitude increase in ME coupling and larger voltage output can be realized.[6–9] The signal-to-noise ratio of these resonant sensors can be enhanced by increasing the sensitivity or by lowering the equivalent magnetic noise floor. The resolution of sensors driven at resonance is limited, in particular, by the mechanical quality factor Q. However, a large value of Q also narrows the bandwidth. Broadband operation can still be achieved if an applied magnetic field modifies the stress in a magnetostrictive or ME resonator and thereby tunes the resonance.[8–11]

This approach has previously been demonstrated in clamped-clamped ME bimorphs with Metglas and FeNi (Ref. 6) as well as in ME cantilevers, where the shift in frequency f is related to the ΔE effect.[7] Stress reconfigurable doubly clamped magnetostrictive resonators offer the possibility for near-DC magnetic field sensing by determining the magnetic field induced shift in the resonant frequency f_R resulting from a change in stress owing to magnetostriction.[11] In this scheme, it is possible to minimize the impact of $1/f$ noise and thus lower the equivalent magnetic noise floor by increasing f_R via decreasing the device size. The use of MEMS fabrication techniques to create these structures allows for standardized production of sensor arrays as well as integration with other CMOS components.

With this stress reconfigurable approach, it is now possible to increase the Q and enhance resolution without sacrificing bandwidth. Several parameters can affect the Q of a mechanical resonator such as thermoelastic losses, clamping losses, and surface effects like defects or surface roughness.[12] However, air damping has been established as the foremost limitation on Q as the volume-to-surface ratio of the resonator decreases.[13] Reducing contributions from air damping by operating micromechanical cantilevers in vacuum can therefore significantly increase Q by several orders of magnitude.[14,15] Furthermore, ME composite cantilevers under vacuum showed an increase in ME coupling and a lowered limit of detection for magnetic field sensing.[15] Yet similar studies have not been performed on doubly clamped reconfigurable sensors that are expected to have higher f_R, and consequently, enhanced Q. It is also desirable to lower the limit of detection and improve the resolution and sensitivity by increasing Q, while maintaining the tunability of these devices.

We have recently fabricated stress reconfigurable magnetoelastic CoFe thin film sensors and demonstrated a change in the bending mode resonant frequency with applied field perpendicular to the length of the bridges as well as improved magnetic field sensitivity as compared to large scale devices.[9] In this work, we examine and verify the stress induced origin of this anisotropy as well as investigate the pressure dependence of the Q of these sensors.

$Co_{68}Fe_{32}$ free-standing resonators were fabricated on Si substrates, as previously described.[9] A length of 1 mm was chosen based on fabrication techniques and targeted resonant frequency. Longitudinal magneto-optic Kerr effect (MOKE) was used to measure the in-plane angular dependence of magnetic hysteresis loops on the free standing resonators at room temperature in atmospheric conditions. A rotation stage with *x-y* adjustment ensured accurate alignment of the laser beam with the resonators. For measurements of resonance, a $PbZr_{1-x}Ti_xO_3$ (PZT) piezoelectric transducer was used to drive the vibration of the sample [schematic of sample is shown in Figure 1(a)]. This structure was placed in a small vacuum chamber between the poles of an electromagnet for measurements with applied magnetic field (H) at different background pressures. The transverse displacement of an individual beam was measured with a laser Doppler vibrometer (LDV) (Polytec OFV-5000). This signal was processed by a lock-in amplifier (Signal Recovery 7280) to determine the amplitude A. The f_R and Q were obtained by fitting the frequency dependent amplitude with $A(f) = A_0 f_R^2 ((f^2 - f_R^2)^2 + f^2 f_R^2 Q^{-2})^{-1/2}$ for damped driven simple harmonic oscillation, where A_0 is the amplitude of the excitation.[16,17]

The resonance peaks with an in-plane H applied both parallel (defined as 0°) and perpendicular (90°) to the length of the beam are shown in Figures 1(b) and 1(c), respectively. Although a change in amplitude is immediately apparent for H along 0°, no shift in f_R is observed as opposed to the clear increase in frequency of about 1.5 kHz when H is perpendicular to the beam. To further investigate this interesting anisotropic magnetic response, longitudinal MOKE measurements for a single beam (as shown in Figure 1) were performed. These hysteresis loops reveal that the remnant magnetization normalized to saturation magnetization (M_R/M_S) is decreased from 0.95 at 0° to 0.49 at 90°, where the angle is defined relative to the beam axis. This is in contrast to the hysteresis loops of the CoFe film on the edges of the beam structure (not shown), which did not show a significant difference with 90° rotation. This clearly indicates that the easy magnetization axis is parallel to the length of the beams, whereas the data for H perpendicular to the beam length displays some characteristics of a hard axis. These results are consistent with the expected strong uniaxial stress-induced anisotropy $K_\sigma = (3/2)\,\sigma\lambda_s$, where σ is the stress and λ_s is the saturation magnetostriction, $\sim$20 kJ/m^3 even with a conservative value of λ_s of FeCo $\lambda \sim 40$ ppm. This is larger than the demagnetization energy in the plane of the beam, which is calculated[18] to be 12 kJ/m^3. The in-plane angular dependence of the coercive magnetic field (H_C) shows a sharp increase with applied magnetic field at precisely 90° and is qualitatively consistent with the Kondorsky model of 180° domain wall growth and propagation through the film.[19,20]

The resonant mode [Figure 2(a)] displays a dependence on pressure P. The value of f_R is found to increase with decreasing pressure (not shown), and this shift, consistent with previous reports,[14,21] is attributed to the reduction of inertia of the air moved by the beam.[22]

For the peaks shown in Figure 2(a), Q increased from $\sim$103 at atmospheric pressure to $\sim$2728 at 1 Torr. Two distinct regimes can be seen in the P dependence of the Q [Fig. 2(b)] with a large jump in Q at lower pressure P, reaching over 8000 at 85 mTorr. The total quality factor from all of the damping parameters present sums as $\frac{1}{Q_{eff}} = \sum_i \frac{1}{Q_i} = \frac{1}{Q_{air}} + \frac{1}{Q_{intrinsic}}$, where Q_{air} is the quality factor related to damping by air and $Q_{intrinsic}$ is that due to the device. Air damping is the dominant mechanism in micromechanical systems until it becomes comparable to intrinsic damping at very low pressures,[13,14] and therefore, Q_{eff} is controlled by how the drag force is determined in different pressure ranges.

Near atmospheric pressure, air must be treated as a viscous fluid. Due to the difficulty of obtaining analytical solutions for the Navier-Stokes equation for an oscillating beam, Hosaka *et al.*[23] have approximated a resonating beam as a string of independently vibrating spheres of radius r to give

$$Q_{visc} = \frac{\omega \rho_{CoFe} w t}{3\mu(1 + w/\delta)}, \tag{1}$$

where ω is the resonant frequency of the beam, ρ_{CoFe} is the density of the cantilever (8370 kg/m^3), w is the beam width ($\sim$40 μm), t is the beam thickness ($\sim$200 nm), μ is the

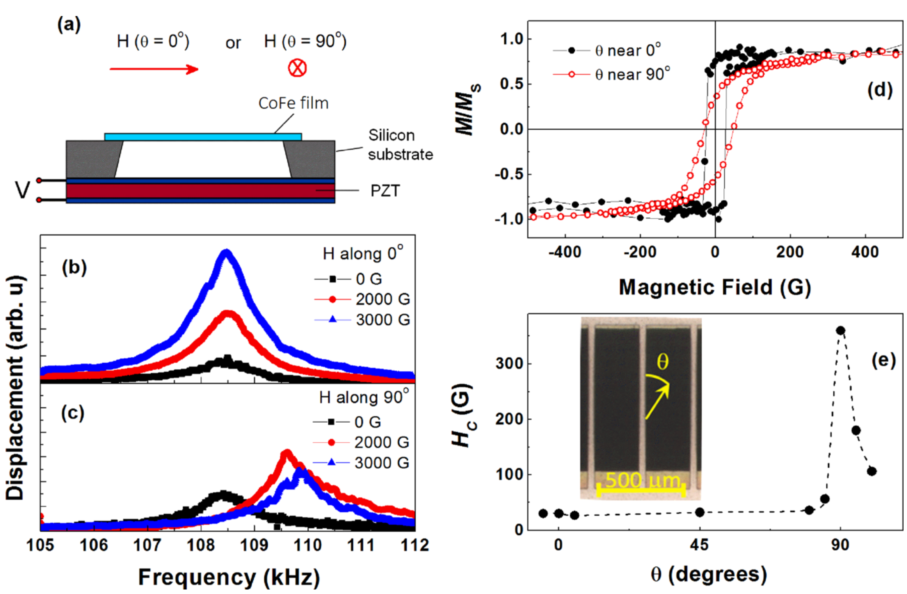

FIG. 1. (a) Schematic diagram showing the structure consistent of a CoFe film that has been patterned on a silicon substrate and back-etched resulting in free-standing beams. This is backed by a PZT stack. (b) The frequency dependent displacement at several magnetic fields applied parallel to the length of the beam (0°) and (c) perpendicular to the beam (90° in-plane). (d) Representative magnetic hysteresis loops from magneto-optical Kerr effect measurements for a CoFe bridge with magnetic field applied near zero and 90 degrees (±10°). (e) Angular dependence of the coercive field. Angle is defined with respect to the length of the bridge, as shown in the inset.

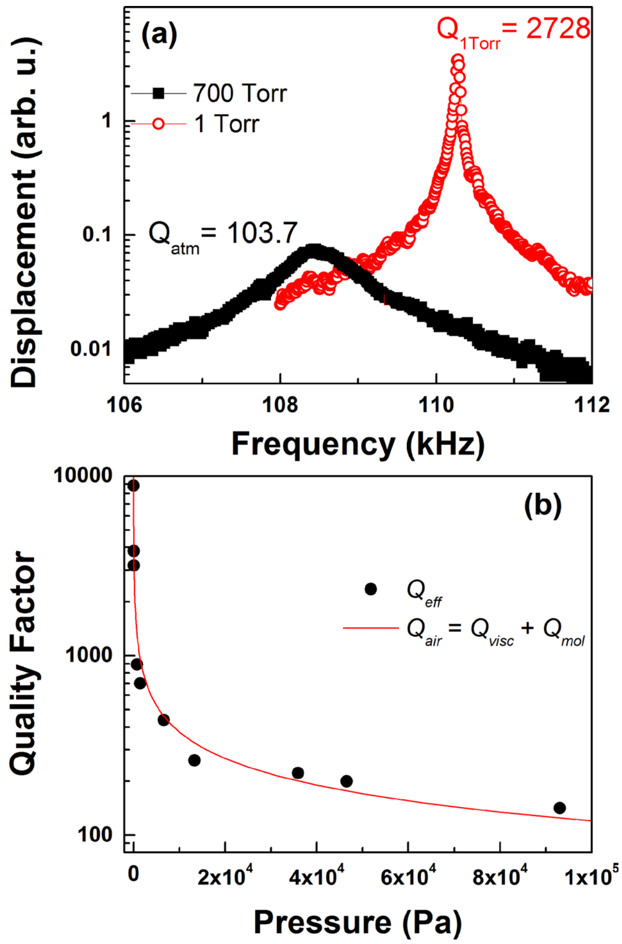

FIG. 2. (a) The mechanical resonance of one of the present CoFe beams at 700 Torr and 1 Torr. A shift in resonant frequency is observed, and the quality factor Q_{eff} is enhanced at low pressures. (b) The pressure dependence of Q_{eff} for the present beam. The data are fitted by combining Eqs. (2)–(4).

viscosity of air, and $\delta = (2\mu/\rho_o\omega)^{1/2}$ with ρ_o being the P-dependent density of air. Zhang and Turner[24] have generalized this expression and shown that

$$Q_{visc} = \frac{\omega\rho wt}{3\mu(a + bw/\delta)}, \tag{2}$$

where a and b are related to both the surface area perpendicular to the direction of motion and the surface area of the sides of the beam. For their measurements, they found that $a \ll b$.

At lower P, where the mean free path is large as compared to the motion of the beam, the air molecules can now be considered as non-interacting and the effects of air damping can be treated as independent collisions of air molecules with the moving surface of the beam. This is the molecular damping regime, and the damping parameter in this region follows from kinetic theory of gasses. For this lower pressure region, Christian has shown that[14,15,25]

$$Q_{mol} = \frac{\omega\rho_{\mathrm{CoFe}}d}{4}\left(\frac{\pi}{2}\right)^{1/2}\sqrt{\frac{RT}{M_{air}}\frac{1}{P}}, \tag{3}$$

where R is the gas constant, M is the molecular mass of air, and T is the temperature (300 K). To model the transition between these two regimes, Lübbe *et al.* have successfully shown that one can consider these as analogous to two resistors in parallel.[16] That is, we consider

$$Q_{air} = Q_{mol} + Q_{visc}. \tag{4}$$

Figure 2(b) shows that by combining Eqs. (2)–(4), the model fits the $Q(P)$ data for the present resonator very well with the only two free parameters $a \sim 0$ and $b = 0.21$. The value of $Q_{intrinsic}$ for clamped beams is expected to be larger than that for a cantilever with identical dimensions as f_R will be higher due to stress developed during processing, as well as $Q_{support}$ is theoretically predicted to increase for clamped-clamped versus clamped-free boundary conditions.[26] In addition to the present results showing a sharp increase in Q in the molecular regime, the enhancement of $Q_{intrinsic}$ for the present stress reconfigurable beams would suggest that Q in ultra-high vacuum could be considerably higher than that for cantilever devices.

For use of these stress reconfigurable devices as magnetic field sensors, it is important to also investigate the effects of H on f_R at various pressures. Figure 3 shows the shift in resonance at 700, 100, and 1 Torr which correspond to the viscous, intermediate, and molecular damping regimes, respectively. The increase in Q as noted previously appears to contribute to an improvement in the signal-to-noise ratio at 1 Torr as compared to that at atmospheric pressure. The effects of magnetic field and pressure are expected to be decoupled, as the magnetostriction-induced stress should be independent of pressure and of a different nature than the shift in f_R due to a change in effective mass with pressure. Thus, the apparent difference in df_R/dH [Fig. 3(d)] is not intrinsic but rather a result of increased resolution at lower pressures due to higher Q, which is consistent with the data appearing noisier and the peak less sharp at atmosphere than at lower pressures.

We previously demonstrated that intrinsic magnetic noise (b_n) of the bridge can be determined by the thermomechanical noise as calculated by the following equation:

$$b_n = \frac{\mu_0}{2}\left(\frac{df_R}{dH}\right)^{-1}\sqrt{\frac{2\pi k_B T f_R}{QV\sigma}}, \tag{5}$$

where V is the volume of the device, and the stress σ is calculated from f_R assuming each bridge is treated as a one-dimensional string.[9,27] From the experimentally determined values of field sensitivity df_R/dH, f_R, and Q, at room temperature and atmospheric pressure, the calculated value of b_n is assessed to be 155 pT/$\sqrt{}$Hz, which is consistent with our previous results. As the pressure is decreased to 1 Torr, Eq. (5) predicts that the intrinsic magnetic noise is reduced by a factor of 6 ($b_n \sim 25$ pT/$\sqrt{}$Hz). These values suggest that encapsulating the present sensors in vacuum will result in enhanced performance of these devices as magnetic field sensors. In addition, by fabricating a magnetoelectric composite by integrating a piezoelectric layer with the CoFe beams, decreasing the pressure is also expected to increase the resonant magnetoelectric coupling and the induced voltage, thereby further improving the limit of detection.[15] Measurements of the equivalent magnetic sensor noise are under progress. The effects of further miniaturization of the beams or mitigation

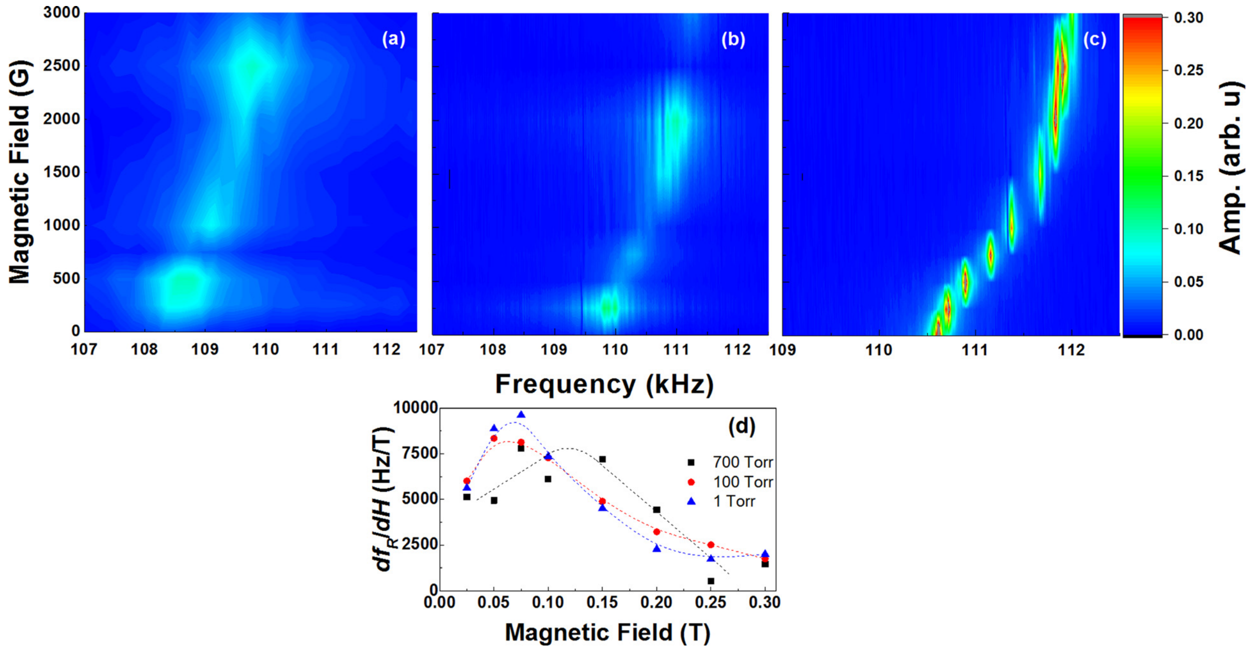

FIG. 3. The magnetic field dependence of resonant frequency (a) 700 Torr, (b) 100 Torr, and (c) 1 Torr. (d) The magnetic field sensitivity of the resonant frequency f_R at various pressures. The dashed lines are a guide for the eye.

of internal stress from processing on the equivalent magnetic noise floor would also be of interest in establishing the range of useful device sizes and optimal fabrication processes.

In summary, it was determined that the easy magnetization axis of CoFe free-standing thin film resonators is aligned with the length of the beams due to a combination of stress and shape anisotropy. The mechanical quality factor was enhanced under vacuum, which could contribute considerably to an increase in signal-to-noise ratio of the sensor and improve magnetic field sensitivity. A significant reduction in the intrinsic magnetic noise is also predicted, making these stress reconfigurable sensors a promising candidate for near DC magnetic field sensing.

Funding for this project was provided by the Office of Naval Research (ONR). The work of M.S. at the Naval Research Laboratory was supported in part by the National Research Council under the Research Associateship Program.

[1]Y. Wang, J. Li, and D. Viehland, Mater. Today **17**, 269 (2014).
[2]J. Zhai, Z. Xing, S. Dong, J. Li, and D. Viehland, Appl. Phys. Lett. **88**, 062510 (2006).
[3]T. Uchiyama, K. Mohri, Y. Honkura, and L. V. Panina, IEEE Trans. Magn. **48**, 3833 (2012).
[4]V. Kumar, M. Mahdavi, X. Guo, E. Mehdizadeh, and S. Pourkamali, in *Proceedings of the 28th IEEE International Conference on Micro Electro Mechanical Systems* (2015), pp. 204–207.
[5]N. A. Stutzke, S. E. Russek, D. P. Pappas, and M. Tondra, J. Appl. Phys. **97**, 10Q107 (2005).
[6]P. Finkel, J. Bonini, E. Garrity, K. Bussman, J. Gao, J. F. Li, S. E. Lofland, and D. Viehland, Appl. Phys. Lett. **98**, 092905 (2011).
[7]B. Gojdka, R. Jahns, K. Meurisch, H. Greve, R. Adelung, E. Quandt, R. Knöchel, and F. Faupel, Appl. Phys. Lett. **99**, 223502 (2011).
[8]J. Kiser, P. Finkel, J. Gao, C. Dolabdjian, J. Li, and D. Viehland, Appl. Phys. Lett. **102**, 042909 (2013).
[9]J. Kiser, R. Lacomb, K. Bussmann, C. J. Hawley, J. E. Spanier, X. Zhuang, C. Dolabdjian, S. Lofland, and P. Finkel, Appl. Phys. Lett. **104**, 072408 (2014).
[10]R. Osiander, S. A. Ecelberger, R. B. Givens, D. K. Wickenden, J. C. Murphy, and T. J. Kistenmacher, Appl. Phys. Lett. **69**, 2930 (1996).
[11]C. A. Grimes, C. S. Mungle, K. Zeng, M. K. Jain, W. R. Dreschel, M. Paulose, and K. G. Ong, Sensors **2**, 294–313 (2002).
[12]O. Ergincan, G. Palasantzas, and B. Kooi, Phys. Rev. B **85**, 205420 (2012).
[13]W. E. Newell, Science **161**, 1320 (1968).
[14]F. R. Blom, J. Vac. Sci. Technol., B **10**, 19 (1992).
[15]C. Kirchhof, M. Krantz, I. Teliban, R. Jahns, S. Marauska, B. Wagner, R. Knöchel, M. Gerken, D. Meyners, and E. Quandt, Appl. Phys. Lett. **102**, 232905 (2013).
[16]J. Lübbe, M. Temmen, H. Schnieder, and M. Reichling, Meas. Sci. Technol. **22**, 055501 (2011).
[17]D. A. Walters, J. P. Cleveland, N. H. Thomson, P. K. Hansma, M. A. Wendman, G. Gurley, and V. Elings, Rev. Sci. Instrum. **67**, 3583 (1996).
[18]A. Aharoni, J. Appl. Phys. **83**, 3432 (1998).
[19]E. Kondorsky, J. Phys. **2**, 161 (1940).
[20]L. Sun and H. Xing, J. Appl. Phys. **104**, 043904 (2008).
[21]M. Christen, Sens. Actuators **4**, 555 (1983).
[22]F. Elmer and M. Dreier, J. Appl. Phys. **81**, 7709 (1997).
[23]H. Hosaka, K. Itao, and S. Kuroda, Sens. Actuators, A **49**, 87 (1995).
[24]W. Zhang and K. Turner, Sens. Actuators, A **134**, 594 (2007).
[25]R. G. Christian, Vacuum **16**, 175 (1966).
[26]Z. Hao, A. Erbil, and F. Ayazi, Sens. Actuators, A **109**, 156 (2003).
[27]X. Zhuang, M. L. C. Sing, C. Dolabdjian, P. Finkel, J. Li, and D. Viehland, IEEE Sens. J. **14**, 150 (2014).